Defining Vehicle Passing Trajectories utilizing GNSS Data

Stergios Mavromatis, Vassilios Matragos, Nikolaos-Panagiotis Trantas, Vangelis Zacharis

National Technical University of Athens, Department of Transportation Planning and Engineering
5, Iroon Polytechniou str., GR-15773 Athens, Greece, stemavro@central.ntua.gr

Abstract

The objective of this paper is the investigation of vehicle's passing paths from the road-engineering point of view, with special emphasis on the two pairs of consecutive reverse curved sections at the beginning and ending phase of the passing maneuver respectively. The authors by examining these curved paths intend to quantify their trajectories. The assessment is based on a real-driving experiment, where a realistic representation of the passing task with respect to roadway's posted speed was performed.
The curved paths were determined for two different and mostly typical posted speed values (90km/h and 110km/h), where the impeding (passed) vehicle was assumed to travel under steady state conditions (20km/h below the respective posted speed values). The authors, besides the geometry of the curved passing paths, investigate respective critical parameters, such as headway distance and acceleration performance.
In view of the imminent vehicle automation, although more advanced communication between vehicles or between vehicles and road environment seems a prerequisite in order integrated guidance during passing maneuvers to be enabled, the present research is an opening paradigm of how the passing process can be standardized and therefore deployed in future advanced driver assistance systems.

Keywords: Passing Path, Passing Maneuver, Spiral Curves

1. Introduction and Problem Statement

In general, there are two discrete maneuvers that a vehicle can execute while traveling on a two way lane road; lane keeping and lane changing. Lane keeping has been extensively studied the past years [1], where modules that automate such a driving task are being incorporated in recent consumer vehicles. However, the lane changing maneuver is not yet adequately modeled and remains a cutting edge research topic in the global scientific community. Even more so does the overtaking process, as it is comprised of two successive lane changing maneuvers.

During lane keeping maneuvers, the vehicle has only one degree of freedom; speed variation operations in the longitudinal direction of travel. On the other hand, lane changing maneuvers are by far more complex, since the vehicle has two degrees of freedom. More specifically, the driver should alter the vehicle's trajectory both in the longitudinal and lateral directions, by adjusting concurrently the speed and the steering angle respectively. By superimposing these two motion components, the resulting trajectory deviates from that of the road geometry.

In addition to plain lane changing maneuvers, during overtaking the passing vehicle enters the opposite traffic lane, where in total three distinct, successive and independent maneuvers are executed; namely, a left lane change, a tangent motion and a right lane change [2, 3, 4, 5, 6, 7, 8, 9].

In general the overtaking and lane change maneuvers are not clearly distinguished in the existing literature. Moreover, when studying mathematical models for the trajectory of the passing vehicle, the published research on the lane change maneuvers could also be used to extrapolate conclusions on the overtaking maneuver.

The forthcoming Advanced Driver Assistance Systems (ADAS) in the near future are expected to address more accurately the passing process and thus standardize vehicle passing paths more accurately. This will be accomplished by defining a virtual overtaking path, or a "Virtual Desired Trajectory" (VDT), that will act as a shadow target for the vehicle to follow during the execution of the maneuver.

In order to define such an optimal trajectory, the proposed algorithms should be harmonized with driver's safety and comfort for rather extensive combinations of spatial coordinates, since two problems need to be addressed. On one hand, the computational complexity of such an effort would be colossal and the module surely will not be efficient enough for real time application, excluding of course emergency situations (e.g. unexpected events that cancel the maneuver). On the other, the numeric values of the parameters of the resulting trajectory might not comply with the accepted thresholds in terms of road safety.

As a result, various methods for defining the VDT have been proposed, which however address the above issues from different standpoints.

The most prominent methodologies for the execution of lane changing maneuvers is the geometric method. It involves a predefined parametric mathematical curve and a dataset of recorded vehicle trajectories. The curve parameters are quantified by statistical means. Various geometric curves have been proposed to serve as the kernel of said mathematical models, such as polynomial expressions of 3rd order [2, 8, 10], 4th order [11], 5th order [3, 11, 12, 13] and 6th order [12], circular arcs [14], sigmoids [15, 16], Bezier curves [17] and spiral arcs (clothoids) [18].

The utilized dataset to quantify the geometric parameters of the curves, can be acquired by conducting a simulator-based or a field-driving experiment. Various researchers use cameras to record overtaking maneuvers unbeknownst to the road users [19, 20, 21], where the vehicle trajectories are deduced after processing the videos with specialized software. In addition, lane changing maneuvers of the surrounding vehicles have been recorded by driving an experimental vehicle mounted with ranging and recording instruments around a predefined path [22, 23]. Another method utilized to record a vehicle's trajectory during lane changing is by means of GNSS receivers [24].

The simulator-based experiments provide the researchers with a safe environment to investigate more complex and risky maneuver scenarios where the overtaking process is not an exception [14, 25, 26]. However, some researchers question the validity of the findings of simulator experiments, as they believe that the participating drivers may execute the maneuvers more aggressively inside a protected bubble [27].

Last but not least, it is almost unanimously proposed that a VDT should always feature a continuous curvature profile, otherwise road safety, passenger comfort and realization of the maneuver are compromised [28, 29, 30, 31, 32].

Spiral curves are mathematical curves with a linearly changing curvature profile widely utilized in current road design practice. Noticing a lack of previous quantification attempts to fit spirals in existing experimental data, the present research aims to develop a new mathematical model for the overtaking maneuver that incorporates a series of successive parametric spiral arcs. A field-driving experiment was conducted to record passing maneuvers by means of GNSS receivers and an overtaking trajectory database was created, which in turn served for the quantification of the spiral curves and the design of predictive models.

2. Methodology

The analysis assumes free flow conditions, where the passing maneuvers were performed on tangent sections of two lane rural roads. Although the passing process includes the contribution of three vehicles; namely the passing vehicle, the passed vehicle and the opposing vehicle, in the simulation experiment the opposing vehicle was ignored. The present paper addresses accelerated passing maneuvers.

Passing maneuvers comprise of 3 segments (Figure 2); in Segment 1 (1st reverse curve) the vehicle is assumed to move gradually from the original driving lane to the opposing lane, in Segment 2 the vehicle travels along the opposing lane (tangent), and in Segment 3 the vehicle returns once more gradually to the original lane (2nd reverse curve). For Segment 1 and Segment 3, the optimal trajectory algorithm is to obtain a trajectory curve starting from the centerline of the current position (lane) to the centerline of the target lane [10].

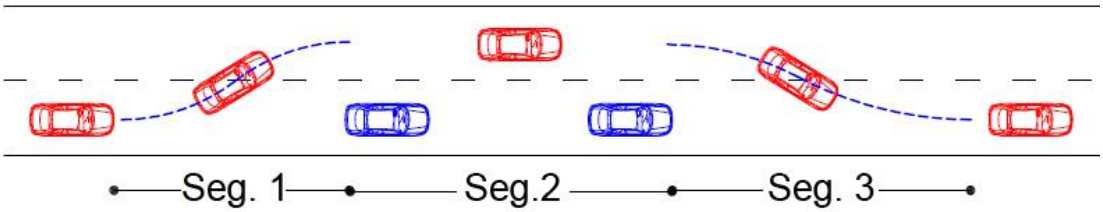

Figure 1: Phases during Passing Maneuvers

The two involved vehicles had different motion characteristics, where the following criteria – assumptions were applied:

- the speed of both vehicles were supposed to never exceed the posted speed of the roadway
- passing maneuvers under 2 different posted speed values were examined; namely, 90km/h and 110km/h
- the motion of the passed vehicle was under steady state conditions with a speed value 20km/h below the posted speed of the roadway
- the passing vehicle's motion during the overtaking process was under acceleration mode; however, it's initial speed value at the starting phase was set equal to the relevant speed of the passed vehicle and increasing continuously until the roadway's posted speed was reached from which point beyond steady state conditions apply

2.1. Driving Experiment

The road experiment took place on an urban divided freeway, under free flow conditions, in Attica prefecture. For safety reasons, the time of the measurements was chosen so that the traffic volumes to be low.

Although the authors acknowledge that the road environment (divided freeway) was not the most appropriate for the experiment, safety reasons made it inevitable. On the other hand, the experiment was based on defining the passing trajectories and not assessing critical issues related to overtaking on two-lane rural roads (e.g. passing sight distance).

The experiment consisted of a 16km long driveway with three lanes (3x3.50m wide) per direction of travel, with both tangents and curves. The overtaking attempts were performed on the middle lane (the impeding vehicle was continuously positioned on the external lane). The participants were asked to drive 3 times including one lap for warming up and getting acquainted with the driving environment. For every one of the two remaining runs a different posted speed was implemented (90km/h and 110km/h), where the speed of the preceding vehicle was

constantly set 20km/h below (70km/h and 90km/h respectively). For every run, the duration of which was approximately 22min, the participants were able to perform between 7 and 9 passing maneuvers.
Moreover, the participants were asked to comply with the predefined posted speed values and perform overtaking maneuvers only on tangents.
During the experiment, the trajectories of both the passing and the impeding vehicles were recorded with high accuracy, using a GPS receiver mounted at the roof of each vehicle. It was decided to use low-cost, u-blox type, GNSS receivers, as they are all-weather devices, designed especially for field measurements.
The collected data were analyzed using the open source RTKLIB suite [33] in differential processing mode. DIOP station at Dionysos Satellite Observatory (DSO) [dionysos.survey.ntua.gr] was used as reference which was streaming GNSS data in RTCM3 format [34] at a rate of 10Hz. Precise orbits and clock corrections were provided from International GNSS Service (IGS) [35] in SP3 and clock RINEX formats respectively.
During the analysis, the default models were used for the modelling of the atmosphere (troposphere and ionosphere) and a combination filter (forward and backward) was used to ensure most of the ambiguities were resolved.
The results were exported in the NMEA0183 standard [36], which provides the vehicle's instantaneous position, as well as its instantaneous velocity, at high accuracy utilizing the Doppler effect measurements on the GNSS satellites. These positions were subsequently transformed from latitude-longitude to projection coordinates (X, Y) in the Greek Geodetic Reference System of 1987 (GGRS87).
In total 170 valid accelerated passing maneuvers were recorded from 32 participants aged between 21 to 58 years old. 19 of the participants were males (mean age 27years) and 13 females (mean age 24years) with mean driving experience 8 years and 4 years respectively. The participants had no known health or vision problems, held a valid driving license and were rather frequent drivers (reported driving more than 3 times per week and more than 5,000km travelled annually).

2.2.Azimuth Diagram

The geometry of the vehicle trajectories during the passing process was defined by drawing the azimuth diagram [14], utilizing the X and Y coordinates of the vehicle path. The azimuth diagram, through regression analysis, defines the angular change rate of the vehicle path along with the driven distance, thus enabling the definition of core design elements (tangents, circular arcs and spiral lengths). More specifically, between two points of vehicle travel length a horizontal line, an inclined line and a curved section (quadratic parabola) define tangent length, circular arc and spiral length respectively.
Thus, for each passing maneuver in the database, the azimuth diagram was created. Figure 2 shows such an example associated with the horizontal alignment of a typical passing maneuver trajectory.
As shown in Figure 2b, a passing maneuver consists of two lane changes, where in between lies a tangent. In the azimuth diagram (Figure 2a), on the other hand, a descending and ascending angular change rate describes leftcurved and rightcurved sections respectively, where the horizontal section stands for tangents. Therefore, it was considered that an overtaking process consists of five distinct phases, as shown through Figure 2(a,b).
The definition of the individual phases were based on the following fundamental assumption: the ending section of the previous phase is tangentially connected with the starting section of the next. In addition, Phase 3 was defined as the interval between the ending point of Phase 2 and the starting point of Phase 4. As a result, Phase 3 sometimes had rather reduced length, which however, did not affect the statistical analysis that followed.
Therefore, for each overtaking it was necessary to identify a total of six points of interest. These are the starting and the ending points of Phase 1, the ending point of Phase 2, the starting and ending points of Phase 4 and the ending point of Phase 5.

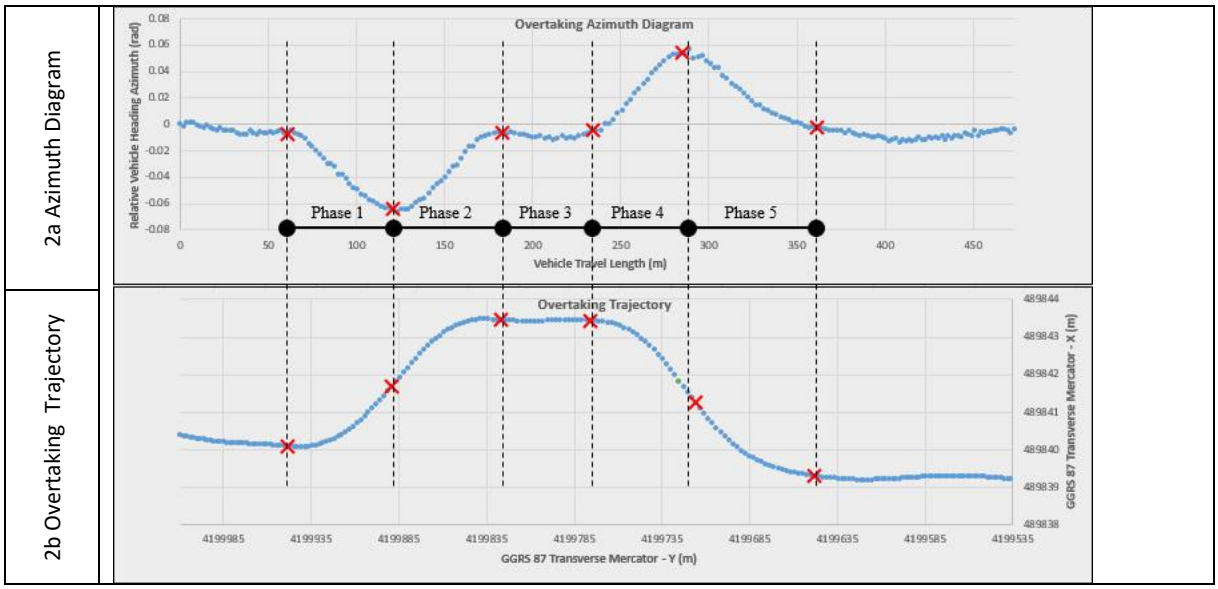

Figure 2(a,b): Separation of overtaking into individual phases based on the azimuth diagram

2.3.Assigning Spiral Curves

Particular emphasis was shown on the behavior of the azimuth diagram near the beginning and ending of each phase. A reverse curved point sequence was noticed in almost all sub-phases, of the entire overtaking data. Therefore, for every Phase, it was decided to adopt a sequence of curve consisting of entry spiral – circular arc – exit spiral. Since between the two spirals in general a curved tangent was not defined, it was decided to eliminate the circular arc length, thus adopting successive spiral lengths. In other words, for each phase the Spiral-to-Curve (SC) transition – Curve-to-Spiral (CS) transition sequence was used [37] where there common point has a common instaneous (point) radius (Figure 3) Such an assumption is not far from the reality, since during an overtaking process the driver constantly alters the steering angle of the vehicle.

In conclusion, a lane shift maneuver was considered to consist of four consecutive spiral curves. If two lane-changing maneuvers are joined together with the use of a tangent, then the mathematical model for describing overtaking maneuver consists of eight spiral curves, divided into two groups of four [18].

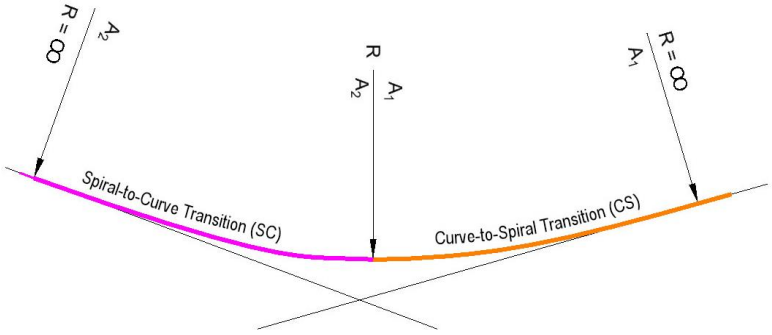

Figure 3: SC transition–CS transition with no inner circular arc [37].

As stated above, each phase consists of two spiral arcs (forming an S-curve), and thus each overtaking phase was divided into two sub-phases. However, this separation point was not specified by the user, as the exact transition point from one sub-phase to the next is not clear in the azimuth diagram.

Contrary to the determination of the transition points between the phases, the internal separation points (in terms of phases) were defined mathematically.

The assumption that the ending section of one phase is tangentially connected to the starting point of the next has been extended to the internal transition points between the two sub-phases of a phase. Given the beginning and ending points of a phase, it was considered that one of the intermediate points of the azimuth diagram was the

boundary point of the respective sub-phases. For every intermediate point, a quadratic polynomial regression was performed for each pair of curves (a and b) and the respective R^2 coefficients corresponding to the two sub-phases (R^2a and R^2b) were also recorded. The procedure was repeated for all intermediate points between the phase boundary points. The combination that gained the maximum value R^2 value ($R^2a + R^2b$) was considered as the most appropriate, as this means that the equations fit better into the actual data and therefore describe them better. The respective point was selected as the separation point of the sub-phases (Figure 4).

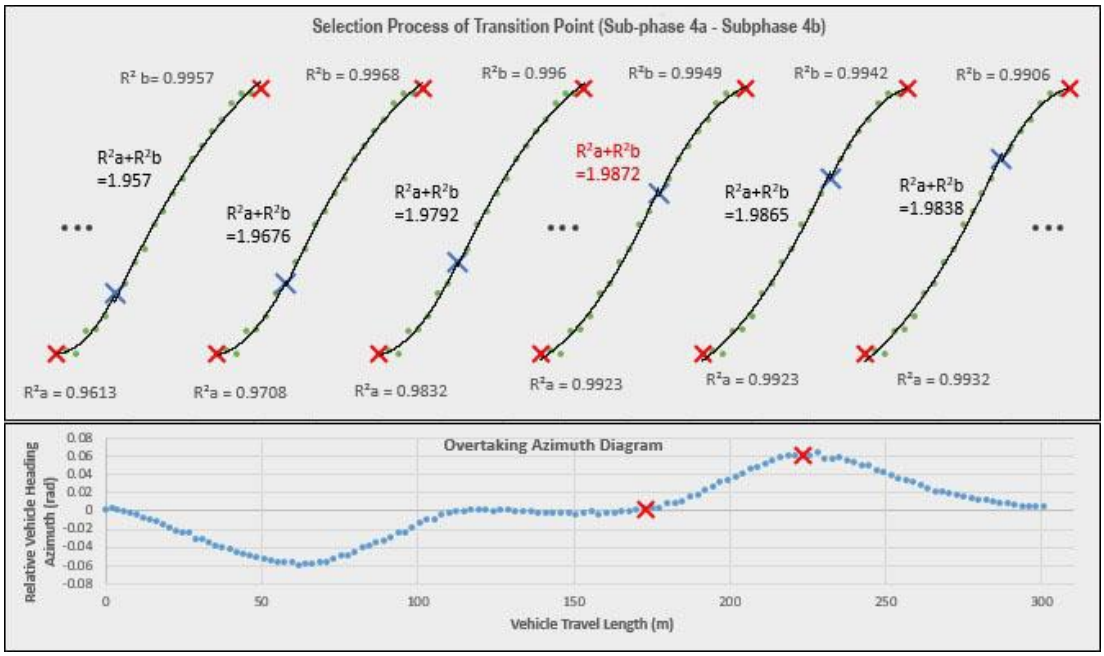

Figure 4: The iterative determination procedure of the transition point between sub-phase 4a and 4b

After defining the four internal separation points of the sub-phases (1a, 1b, 2a, 2b, 3a, 3b, 4a, 4b) the fitting of the trend lines on the azimuth diagram took its final form (Figure 5). The parameters extracted by this spiral curves assessment are the lengths of each spiral curve and the point radius for each Phase. With the utilized polynomial regression the two internal lengths per Phase were determined. As for the point radius, it proves to be independent of the chainage of the transition point from the SC to the CS transition. It was calculated mathematically, using only the total azimuth difference and the total chainage difference during an overtaking phase.

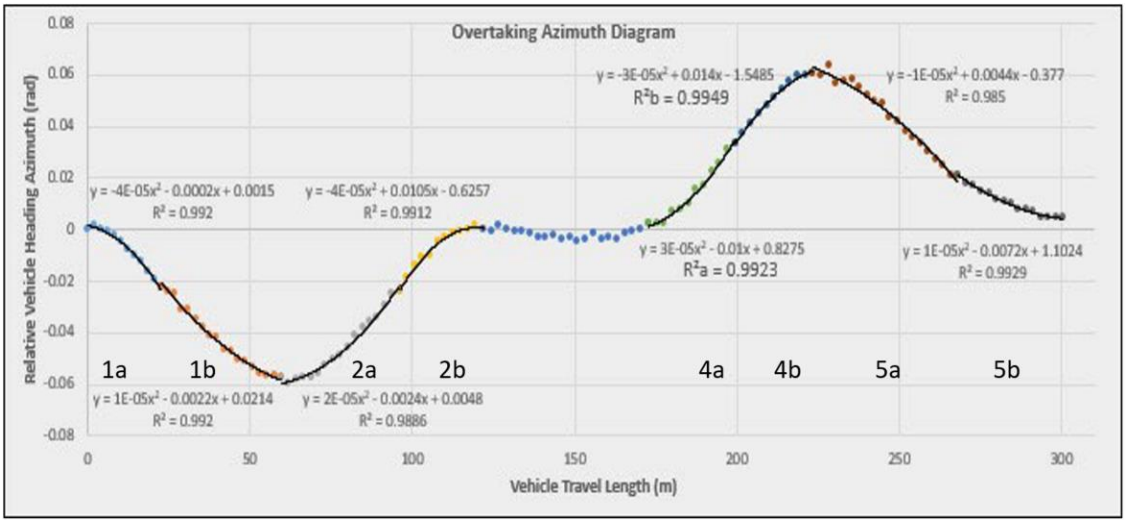

Figure 5: Adjustment of second degree polynomial curves to the azimuth diagram

The mathematical equation used for the radius calculation of each phase is presented as follows:

$$R = \frac{L_{final} - L_{start}}{2(\tau_{final} - \tau_{start})} \qquad (1)$$

where:
R (m) = the (algebraic) point radius between SC and CS transition curves
L_{start} (m) = the chainage of the phase starting point
L_{final} (m) = the chainage of the phase ending point
τ_{start} (rad) = the vehicle azimuth of the phase starting point
τ_{final} (rad) = the vehicle azimuth of the phase ending point

In addition, after determining the internal boundary point of the two sub-phases through the polynomial regression, vehicle azimuth and chainage were calculated. Thus, more parameters for spiral curves could be calculated, for their complete geometric description. (Equations 2-7):

$$A_a = \sqrt{|R| \cdot (L_{middle} - L_{start})} \quad (2)$$

$$A_b = \sqrt{|R| \cdot (L_{final} - L_{middle})} \quad (3)$$

where:
A_a (m) = the parameter A of SC transition curve of sub-phase a
A_b (m) = the parameter A of CS transition curve of sub-phase b
|R| (m) = the absolute value of the point radius
L_{middle} (m) = the chainage of the inner transition point between sub-phase a and sub-phase b

$$L_a = \frac{{A_a}^2}{|R|} = L_{middle} - L_{start} \quad (4)$$

$$L_b = \frac{{A_b}^2}{|R|} = L_{final} - L_{middle} \quad (5)$$

where:
A_a (m) = the parameter A of SC transition curve of sub-phase a
A_b (m) = the parameter A of CS transition curve of sub-phase b
|R| (m) = the absolute value of the point radius
L_{middle} (m) = the chainage of the inner transition point between sub-phase a and sub-phase b

2.4.Dynamic Approach

Along with the investigation of the overtaking maneuver from the road geometry point of view, the research from the dynamic aspect is also of great interest. The present research focused on two parameters, the acceleration of the passing vehicle and the distance between the passing and the impeding vehicle, at the start of the maneuver (headway).

In terms of parameters, for each of the five overtaking phases the mean acceleration of the passing vehicle was calculated. The speeds extracted from the GPS receiver with the form of NMEA0183 Standard [36] were used for the calculation. An assumption was made that the acceleration between two consecutive time frames is constant. In this way, the calculation process was greatly simplified, without any uncertainty in the methodology, since the data recording time frame was most often 0.1s or 0.2s. Thus, the average acceleration per phase was calculated ($a_{i,mean}$).

The headway was calculated at the starting point of the overtaking (start of Phase 1) by the coordinates of the two GPS and the measured lengths between the positon of the GPS and the front or rear bumpers respectively.

2.5.Outputs

As already mentioned, the passing maneuvers were performed assuming two different posted speed values, not to be exceeded (90km/h and 110km/h respectively), where the motion of the impeding (passed) and passing vehicles were under steady state conditions (20km/h below the posted speed) and acceleration, respectively. The authors, aiming to standardize the passing maneuver, for both posted speed values, gave special emphasis to the median values of the boxplot output data, which included: the length and point radii of each overtaking phase, their respective mean acceleration and the total length of the overtaking procedure.

The output data, which refer to the median values of the boxplots for all the overtaking phases, are shown in Figure 6.

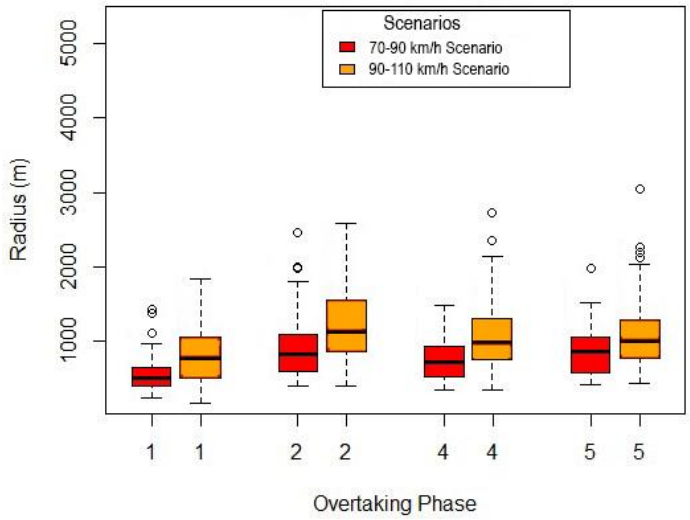

(a) Comparison of Radii

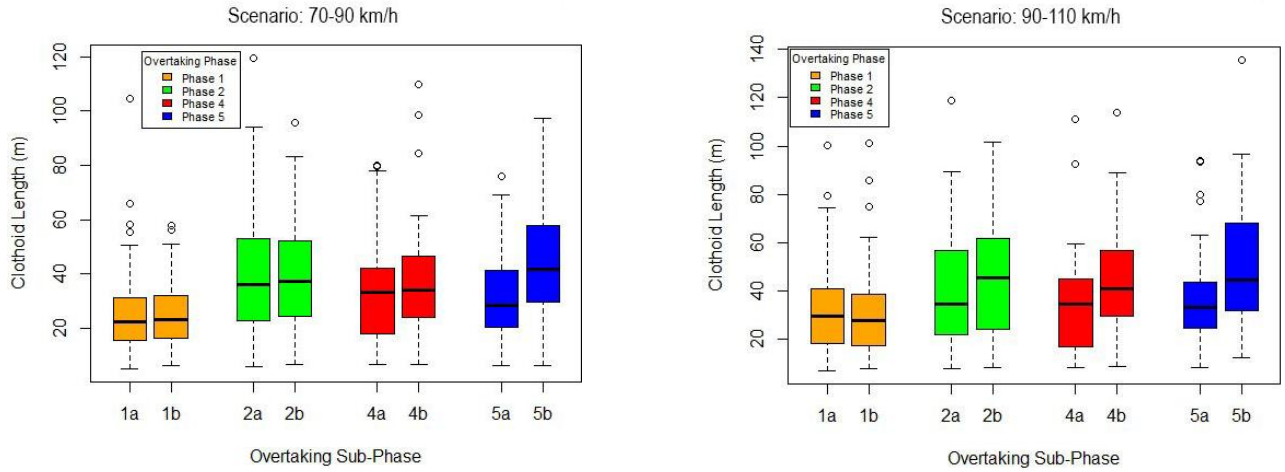

(b) Overview of Lengths

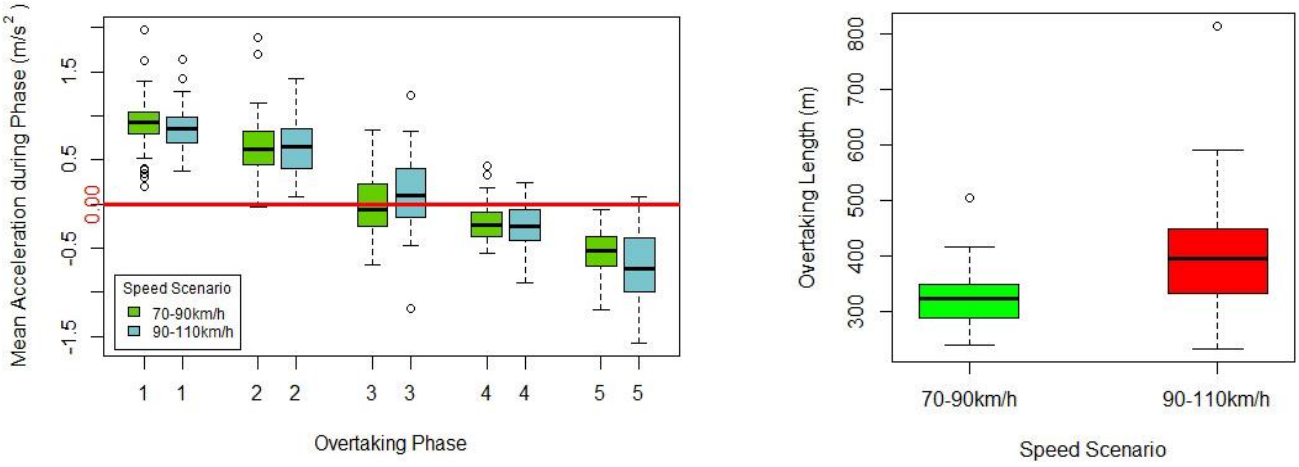

(c) Comparison of vehicle mean acceleration

(d) Total Overtaking Length

Figure 6(a,b,c,d). Passing Data Boxplots during Sub-phases for both scenarios.

3. Discussion and Conclusions

From Figure 6d it is concluded that the speed increases along with the total length required to complete the overtaking maneuver. This implies that the total time required to complete the overtaking remains more or less

constant, regardless of the speed of the two vehicles participating in the maneuver procedure. This is explained by the fact that the difference in the maximum speed of the two vehicles remained constant and equal to 20km/h, but also the acceleration of the passing vehicle, during the first two phases, was about the same in both examined speed scenarios (Figure 6c).

By Figure 13c, it immediately becomes apparent that the passing vehicle accelerated during Phase 1 and Phase 2 overtaking. The zero acceleration during Phase 3 means that the vehicle had reached the maximum speed limit (posted speed/+20km/h compared to impeding vehicle). However, it should be noted the negative acceleration (deceleration) that occurs during Phase 4 and even more so during Phase 5 of the overtaking maneuver.

A very probable explanation has to do with the fact that during Phase 3 the drivers only focused their attention not to exceed the posted speed limit. Although the research team assured the drivers that a deviation of ± 5km/h from the theoretical posted speed was acceptable, the drivers may have been subconsciously afraid to accelerate properly, so to avoid exceeding the speed limit.

It is a fact that the utilization of spiral curves delivers very high coefficients of determination values (R^2>95%) for all examined cases and ensures the continuity of the curvature diagram during the overtaking procedure. In conclusion, and taking into account all above mentioned, the spiral curve assignment of the passing process is strongly recommended as a mathematical simulation to describe and standardize the trajectory of an overtaking maneuver.

A very important subject for further research, would be the integration of the lateral distance between the passing and the impeding vehicle (lateral safety margin) during the structure of overtaking models. In particular, lateral safety margin at the beginning of each phase is expected to show a large correlation with the respective point radii. Also the separation of the dataset, in aggressive and normal driving behavior, in terms of each phase's mean acceleration, would predict the overtaking trajectories more accurately.

Therefore, in terms of vehicle automation, the present analysis addresses mainly cases where only the passing vehicle can be automated (the impeding vehicle conventional). For the above 20km/h speed difference, the research is an opening paradigm of how the passing process can be standardized and therefore deployed in existing ADAS. At present time, this effort is at preliminary stage since the speed of the passed vehicle was considered constant but also traffic conditions were assumed ideal.

An imminent challenge is to further improve the described methodology by enabling more sophisticated communication between vehicles (V2V) or between vehicles and road environment (V2I) and thus enable the utilization of guidance during the passing process in an advanced vehicle automation levels environment. During such an effort, cases of unforeseen situations that might cancel the passing process should be also addressed.

References

1. Lee, J., J. Choi, K. Yi, M. Shin, and B. Ko. Lane-keeping assistance control algorithm using differential braking to prevent unintended lane departures. Control Engineering Practice, 2014. 23:1-13.
2. Zhang, S., W. Deng, Q. Zhao, H. Sun, and B. Litkouhi. Dynamic trajectory planning for vehicle autonomous driving. 2013 IEEE International Conference on Systems, Man, and Cybernetics, October 2013. pp. 4161-4166.
3. Shamir, T.. How should an autonomous vehicle overtake a slower moving vehicle: Design and analysis of an optimal trajectory. IEEE Transactions on Automatic Control, 2004. 49(4): 607-610.
4. Usman, G., and F. Kunwar. Autonomous vehicle overtaking-an online solution. 2009 IEEE International Conference on Automation and Logistics, August 2009. pp. 596-601.
5. Perez, J., V. Milanes, E. Onieva, J. Godoy, and J. Alonso. Longitudinal fuzzy control for autonomous overtaking. 2011 IEEE International Conference on Mechatronics, April 2011. pp. 188-193.
6. Alia, C., T. Reine, and C. Ali. Maneuver planning for autonomous vehicles, with clothoid tentacles for local trajectory planning. 2017 IEEE 20th International Conference on Intelligent Transportation Systems (ITSC), October 2017. pp. 1-6.
7. Yu, Y., A. El Kamel, and G. Gong. Modeling and simulation of overtaking behavior involving environment. Advances in Engineering Software, 2014. 67:10-21.
8. Petrov, P., and F. Nashashibi. Modeling and nonlinear adaptive control for autonomous vehicle overtaking. IEEE Transactions on Intelligent Transportation Systems, 2014. 15(4):1643-1656.
9. Naranjo, J., C. Gonzalez, R. Garcia, and T. De Pedro. Lane-change fuzzy control in autonomous vehicles for the overtaking maneuver. IEEE Transactions on Intelligent Transportation Systems, 2008. 9(3):438-450.
10. Yang, D., S. Zheng, C. Wen, P. Jin, and B. Ran. A dynamic lane-changing trajectory planning model for automated vehicles. Transportation Research Part C: Emerging Technologies, 2018. 95: 228-247.
11. Glaser, S., B. Vanholme, S. Mammar, D. Gruyer, and L. Nouveliere. Maneuver-based trajectory planning for highly autonomous vehicles on real road with traffic and driver interaction. IEEE Transactions on intelligent transportation systems, 2010. 11(3):589-606.

12. Papadimitriou, I., and M. Tomizuka. Fast lane changing computations using polynomials. Proceedings of the 2003 American Control Conference, 2003. 1:48-53.
13. Sazgar, H., S. Azadi, and R. Kazemi. Trajectory planning and combined control design for critical high-speed lane change manoeuvres. Proceedings of the Institution of Mechanical Engineers, Part D: Journal of Automobile Engineering, 2020. 234(2-3):823-839.
14. Karamanou, A., K. Papazissi, D. Paradissis, and B. Psarianos. Precise Estimation of Road Horizontal and Vertical Geometric Features using Mobile Mapping Techniques. 6th International Symposium on Mobile Mapping Technology, São Paulo, Brazil, 2009.
15. Isermann, R., R. Mannale, and K. Schmitt. Collision-avoidance systems PRORETA: Situation analysis and intervention control. Control Engineering Practice, 2012. 20(11):1236-1246.
16. Huang, X., W. Zhang, and P. Li. A path planning method for vehicle overtaking maneuver using sigmoid functions. IFAC-PapersOnLine, 2019. 52(8):422-427.
17. Chen, J., P. Zhao, T. Mei, and H. Liang. Lane change path planning based on piecewise bezier curve for autonomous vehicle. Proceedings of 2013 IEEE International Conference on Vehicular Electronics and Safety, July 2013. pp. 17-22.
18. Wilde, D.. Computing clothoid segments for trajectory generation. 2009 IEEE/RSJ International Conference on Intelligent Robots and Systems, October 2009. pp. 2440-2445.
19. Llorca, C., and A. García. Evaluation of passing process on two-lane rural highways in Spain with new methodology based on video data. Transportation Research Record: Journal of the Transportation Research Board, 2011. 2262:pp. 42-51.
20. Polus, A., M. Livneh, and B. Frischer. Evaluation of the passing process on two-lane rural highways. Transportation Research Record: Journal of the Transportation Research Board, 2000. 1701:53-60.
21. Vetters, A., and T. Jaehrig. Verification of the existing model for passing sight distance on single two-lane rural carriageways. 2015 6th IEEE International Conference on Cognitive Infocommunications (CogInfoCom), October 2015. pp. 557-561.
22. Yao, W., H. Zhao, P. Bonnifait, and H. Zha. Lane change trajectory prediction by using recorded human driving data. 2013 IEEE Intelligent Vehicles Symposium (IV), June 2013. pp. 430-436, pp. 430-436.
23. Carlson, P., J. Miles, and P. Johnson. Daytime high-speed passing maneuvers observed on rural two-lane, two-way highway: Findings and implications. Transportation Research Record: Journal of the Transportation Research Board, 2006. 1961:9-15.
24. Xuan, Y., and B. Coifman. Lane change maneuver detection from probe vehicle DGPS data. 2006 IEEE Intelligent Transportation Systems Conference, September 2006. pp. 624-629.
25. Lu, C., H. Wang, C, Lv, J. Gong, J. Xi, and D. Cao. Learning driver-specific behavior for overtaking: A combined learning framework. IEEE Transactions on Vehicular Technology, 2018. 67(8):6788-6802.
26. Jenkins, J., and L. Rilett. Application of distributed traffic simulation for passing behavior study. Transportation Research Record: Journal of the Transportation Research Board, 2004. 1899:11-18.
27. Llorca, C., and H. Farah. Passing behavior on two-lane roads in real and simulated environments. Transportation Research Record: Journal of the Transportation Research Board, 2016. 2556:29-38.
28. Scheuer, A., and T. Fraichard. Collision-free and continuous-curvature path planning for car-like robots. Proceedings of International Conference on Robotics and Automation, April 1997. pp. 867-873.
29. Connors, J., and G. Elkaim. Analysis of a spline based, obstacle avoiding path planning algorithm. 2007 IEEE 65th Vehicular Technology Conference-VTC2007, April 2007. pp. 2565-2569.
30. Nelson, W. Continuous-curvature paths for autonomous vehicles. Proceedings, 1989 International Conference on Robotics and Automation, May 1989. pp. 1260-1264.
31. Thompson, S., and S. Kagami. Continuous curvature trajectory generation with obstacle avoidance for car-like robots. International Conference on Computational Intelligence for Modelling, Control and Automation and International Conference on Intelligent Agents, Web Technologies and Internet Commerce (CIMCA-IAWTIC'06), November 2005. pp. 863-870.
32. Kanayama, Y., and B. Hartman. Smooth local-path planning for autonomous vehicles. The International Journal of Robotics Research, 1997. 16(3):263-284.
33. RTKLIB: An Open Source Program Package for GNSS Positioning. http://www.rtklib.com/. Accessed April 20, 2021.
34. Wübbena, G., M. Schmitz, and A. Bagge. Real-Time GNSS Data Transmission Standard RTCM 3.0., 2006. https://www.researchgate.net/publication/308634943_Real-Time_GNSS_Data_Transmission_Standard_RTCM_30. Accessed May 2021.
35. IGS Products. https://www.igs.org/products/. Accessed May 16, 2021
36. NMEA 0183 Interface Standard https://www.nmea.org/content/ STANDARDS/ NMEA_0183_Standard. Accessed May 20, 2021.
37. Ministry of Environment, Regional Planning and Public Works. Guidelines for the Design of Road Projects, Part 3, Alignment (OMOE-X), Greece, 2001.